

## Multiple roles of the candidate oncogene *ZNF217* in ovarian epithelial neoplastic progression

Peixiang Li<sup>1</sup>, Sarah Maines-Bandiera<sup>1</sup>, Wen-Lin Kuo<sup>2</sup>, Yinghui Guan<sup>2</sup>, Yu Sun<sup>1</sup>, Mark Hills<sup>3</sup>, Guiqing Huang<sup>2</sup>, Collin C. Collins<sup>2</sup>, Peter C.K. Leung<sup>1</sup>, Joe W. Gray<sup>2,4</sup> and Nelly Auersperg<sup>1\*</sup>

<sup>1</sup>Department of Obstetrics and Gynecology, University of British Columbia, Vancouver, BC, Canada

<sup>2</sup>University of California San Francisco Cancer Center, San Francisco, CA

<sup>3</sup>The Terry Fox Laboratory, BC Cancer Agency, Vancouver, BC, Canada

<sup>4</sup>Life Sciences Division, Lawrence Berkeley National Laboratory, Berkeley, CA

The transcription factor *ZNF217* is often amplified in ovarian cancer, but its role in neoplastic progression is unknown. We introduced *ZNF217*-HA by adenoviral and retroviral infection into normal human ovarian surface epithelial cells (OSE), *i.e.*, the source of ovarian cancer, and into SV40 Tag/tag expressing, p53/pRB-deficient OSE with extended but finite life spans (IOSE). In OSE, *ZNF217*-HA reduced cell-substratum adhesion and accelerated loss of senescent cells, but caused no obvious proneoplastic changes. In contrast, *ZNF217*-HA transduction into IOSE yielded two permanent lines, I-80RZ and I-144RZ, which exhibited telomerase activity, stable telomere lengths, anchorage independence and reduced serum dependence, but were not tumorigenic in SCID mice. This immortalization required short-term EGF treatment near the time of crisis. The permanent lines were EGF-independent, but *ZNF217*-dependent since siRNA to *ZNF217* inhibited anchorage independence and arrested growth. Array CGH revealed genomic changes resembling those of ovarian carcinomas, such as amplicons at 3q and 20q, and deletions at 4q and 18, associated with underexpressed annexin A10, N-cadherin, desmocollin 3 and PAI-2, which have been reported as tumor suppressors. The lines overexpressed *EEF1A2*, *SMAR3* and *STAT1* and underexpressed other oncogenes, tumor suppressors and extracellular matrix/adhesion genes. The results implicate *ZNF217* as an ovarian oncogene, which is detrimental to senescing normal OSE cells but contributes to neoplastic progression in OSE with inactivated p53/RB. The resemblance of the genomic changes in the *ZNF217*-overexpressing lines to ovarian carcinomas provides a unique model to investigate interrelationships between these changes and ovarian neoplastic phenotypes.

© 2007 Wiley-Liss, Inc.

**Key words:** *ZNF217*; oncogene; ovarian cancer; immortalization

The candidate oncogene *ZNF217*, predicted to encode alternatively spliced Krüppel-like transcription factors, was originally identified because of its location in an amplicon on chromosome 20q13.2 in breast cancer cell lines and tumors and by its recurrent expression in other malignancies.<sup>1</sup> *ZNF217* is expressed in normal tissues, and is overexpressed in all cell lines and tumors where the gene locus is amplified.<sup>2</sup> Amplification of 20q, which involves a large number of potentially relevant genes, has since been described in many types of human cancers.<sup>3–10</sup> The 20q region, and *ZNF217* specifically, is amplified in a high proportion of ovarian carcinomas, and expression levels of *ZNF217* correlate with their copy numbers in primary ovarian cancers.<sup>11,12</sup> However, because of the coexistence of other amplified genes in the same region, it has been difficult to define the specific influence of *ZNF217* on malignant progression. An increased copy number of *ZNF217* is associated with reduced survival of ovarian cancer patients.<sup>13,14</sup> In experimental systems, 20q13 amplification has been associated with genome instability and immortalization in cultured human uroepithelial cells.<sup>15,16</sup> Furthermore, overexpression of *ZNF217* in 2 human mammary epithelial cell lines with finite lifespans resulted in the establishment of permanent cell lines with increased telomerase activity, stabilized telomere length and resistance to TGF- $\beta$ -mediated growth inhibition.<sup>17</sup> Recently, *ZNF217* overexpression was found to be associated with resistance to chemotherapy and telomere dysfunction.<sup>18</sup>

We investigated the functional consequences of *ZNF217* overexpression by transducing the gene into human ovarian surface epithelial (OSE) cells, which are thought to be the source of ovarian epithelial carcinomas.<sup>19</sup> Normal OSE cells were investigated soon after explantation into culture and after finite extension of their life span with SV40 Tag/tag (IOSE).<sup>20</sup> Transient adenoviral infection of *ZNF217*-HA into OSE caused selective loss of senescent cells, but no other obvious changes. In 2 separate IOSE lines, retroviral infection with *ZNF217*-HA in conjunction with brief epidermal growth factor/hydrocortisone treatment during crisis gave rise to permanent cell lines with activated telomerase, stable telomere lengths, increased anchorage- and serum-independence and genomic changes resembling those of ovarian cancers. The results support the hypothesis that *ZNF217* contributes to the neoplastic progression of epithelial ovarian carcinomas.

### Material and methods

#### Cell culture

Normal ovarian surface epithelial cells (OSE) were obtained at surgery for nonmalignant gynecological disorders. Ethical permits were obtained as required by the University of BC. The origin of each culture was identified by a hyphenated number. OSE cells in low passage were transfected with SV40 large T and small t antigen (Tag/tag) to give rise to IOSE (“immortalized OSE”), which have an extended but finite lifespan.<sup>20</sup> OSE and IOSE cells were transfected or infected with HA-tagged *ZNF217* constructs and control vectors as described below. The cultures were maintained in medium 199/MDCB105 (Sigma, Mississauga, ON, Canada) with 10% (for OSE) and 5% (for IOSE) FBS (Hyclone, Logan, UT) in humidified 5% CO<sub>2</sub>/air. OSE and IOSE cells senesced after approximately 4–5 and 16–22 passages, respectively. In some experiments, 10 ng/ml epidermal growth factor/1.0  $\mu$ g/ml hydrocortisone (EGF/HC) (Sigma, Mississauga, ON, Canada) was added.

To evaluate the influence of EGF on signal transduction pathways in *ZNF217*-infected IOSE cells that were approaching crisis, cells were grown with and without EGF/HC. Cells grown without EGF/HC senesced by passage 15 and could not be subcultured further. Cells grown in the presence of EGF/HC from passage 14 on could be subcultured twice more to passage 17. Inhibitors of the

This article contains supplementary material available via the Internet at <http://www.interscience.wiley.com/jpages/0020-7136/suppmat>.

Grant sponsor: US Department of Energy, Office of Science, Office of Biological and Environmental Research; Grant number: DE-AC03-76SF00098; Grant sponsor: US National Institutes of Health, NCI P50; Grant numbers: CA 58207; P01 CA 64602; Grant sponsor: National Cancer Institute of Canada.

\*Correspondence to: Department of Obstetrics and Gynaecology, University of British Columbia, BC Women’s Hospital, Rm. 2H30, 4490 Oak Street, Vancouver BC, V6H 3V5, Canada. Fax: +604-875-2725. E-mail: [auersper@interchange.ubc.ca](mailto:auersper@interchange.ubc.ca)

Received 9 May 2006; Accepted after revision 27 July 2006

DOI 10.1002/ijc.22300

Published online 31 January 2007 in Wiley InterScience (www.interscience.wiley.com).

PI3K pathway (20  $\mu$ M LY294002, Calbiochem, San Diego, CA) or the MAPK/ERK pathway (10  $\mu$ M PD98059, Calbiochem), in 199:105/5% FBS with EGF/HC, were added to subconfluent, passage 17 cultures, 24 hr after seeding and daily for 3 days. Then, the cells were lysed in 100  $\mu$ l of lysis buffer (see below). Total protein for each culture was calculated, and the lysates were used for Western blot analysis.

#### *Retroviral infection of ZNF217*

IOSE cells were infected with recombinant retroviruses containing the HA-tagged ZNF217 minigene<sup>17</sup> or empty vector control. The recombinant retroviral vector pLXSN, (BD Biosciences, Mississauga, ON, Canada) containing ZNF217-HA, and empty pLXSN vector were amplified in STBL2 competent cells (Invitrogen) and high titer amphotrophic stocks of ZNF217-HA and control retrovirus were prepared using a transient packaging system. Forty-eight hours after infection, the cells were selected with 150  $\mu$ g/ml G418. G418-resistant cells were pooled after 2–3 weeks, when selection was complete. Infection efficiency was evaluated with the recombinant retrovirus containing EGFP.

#### *Construction of recombinant adenovirus and infection of IOSE cells*

The ZNF217-HA cDNA fragment was cut out from the retroviral vector used earlier with EcoR I enzyme. After electrophoresis, the fragment was isolated and gel-purified before ligating into a recombinant adenovirus pShuttle vector (Clontech Laboratories, Palo Alto, CA). pShuttle clones containing right orientation of ZNF217-HA were confirmed by analyzing restriction digestion patterns and by direct DNA sequence analysis. The cDNA fragment was transferred from the pShuttle vector into an adenoviral vector as per the instruction manual. The recombinant adenovirus containing ZNF217-HA was rescued from packaging 293 cells 2 weeks after transfection. IOSE cells were infected with recombinant adenoviruses (either EGFP or  $\beta$ -galactosidase controls or ZNF217-HA virus) at a concentration of 20 MOI for 1 hr at 37°C and incubated for 24–96 hr before ZNF217-HA gene expression was analyzed. Infection efficiency was evaluated with recombinant adenovirus containing the gene for EGFP.

#### *Immunofluorescence microscopy*

Cells grown on coverslips were rinsed in serum-free medium, fixed in  $-20^{\circ}\text{C}$  methanol, permeabilized 5 min in  $-20^{\circ}\text{C}$  methanol-acetone (1:1), dried, rinsed in PBS, blocked in DAKO (Mississauga, ON, Canada) protein block for 30 min, treated with primary antibody to HA (F-7, Santa Cruz Biotechnology, Santa Cruz, CA) in DAKO protein block 1:400 for 1 hr, rinsed, incubated in secondary antibody (Alexa-594 conjugated goat anti-mouse IgG antibody, Molecular Probes, Eugene OR) in DAKO protein block 1 hr, washed and mounted in Gelvatol.

#### *Array CGH*

Whole genome scanning BAC arrays (HumArray 2.0) composed of 2,464 clones were prepared by the UCSF Array Core.<sup>21,22</sup> Labeling of genomic DNA (CY3- and CY5-dUTP for tumor and female genomic DNA, respectively), array CGH hybridization and image processing were performed as previously described.<sup>22</sup> The CY3, CY5 and DAPI (4', 6-diamidino-2-phenylindole) images were segmented and analyzed to determine CY3/CY5 ratios for each array element using custom software as described.<sup>23</sup>

#### *Affymetrix array analysis*

Total RNA was purified from cells grown to 70–80% confluency with the RNeasy kit from Qiagen by following manufacturer's instructions (Qiagen, Mississauga, ON, Canada). Biotin labeled cRNA was then prepared from purified total RNA according to manuals at www.affymetrix.com. Twenty micrograms of labeled cRNA was hybridized to Affymetrix U133A chips which were later scanned in the genome core facility at the Gladstone

Institute of UCSF. Relative expression levels of probe sets on the arrays were analyzed and calculated by GeneTraffic one color Microarray Data Analysis software (www.ioption.com) using the robust multiarray average (RMA) algorithms.<sup>24</sup> At least 4 samples for each line were analyzed.

#### *RT-PCR*

Total RNA was purified as described earlier. First-strand cDNA synthesis was generated with a first-strand cDNA synthesis kit (Amersham Biosciences, Baie d'Urfe, Quebec). Five micrograms total RNA was denatured at 65°C for 10 min and then chilled on ice. Then, 11  $\mu$ l of bulk first-stand cDNA reaction mix, 1  $\mu$ l of DTT (200 mM), and 1  $\mu$ l of random primer (0.2  $\mu$ g/ $\mu$ l) were added, and the samples were incubated at 37°C for 1 hr. A pair of primers spanning ZNF217 (5'—CCTGCACCGGATAATACAAA—3') and HA-fusion tag (5'—TCTGGCACGTCGTATGGGTA—3') was used to amplify transgene (ZNF217-HA) expression. For the PCR reaction, 2  $\mu$ l of first-strand cDNA was used for amplification in a 50- $\mu$ l reaction volume with a final concentration of 50 mM KCl, 10 mM Tris (pH 9.0) and 200  $\mu$ M dNTPs, 100  $\mu$ M of both forward and reverse primers and 5-U taq polymerase. PCR amplification was carried out as follows: a one time denaturation for 5 min at 94°C; 30 cycles of 30-sec denaturation at 94°C, annealing at 55°C for 30 sec, and extension at 72°C for 1 min, followed by a 10-min final extension at 72°C. PCR products were analyzed by agarose gel electrophoresis.

#### *Anchorage independence*

Cells ( $1.3 \times 10^4$ ) were suspended in 5 ml 0.3% agarose in M199:105 medium with 10% FBS and plated on pre-solidified agarose (0.5%) in 60-mm dishes with grids for colony quantification. After 3 weeks, colonies were sized and counted in triplicate dishes per group.

#### *Serum dependence*

Exponentially growing cells were plated in 96-well strip plates (Corning, NY) at  $2 \times 10^3$  cells/well. Cells were incubated in 199:105 medium with serum concentrations from 0 to 5% and were collected after 7–9 days. At the end of the assays, cells were washed with serum-free medium and fixed with  $-20^{\circ}\text{C}$  methanol for 20 min followed by 3 washes with PBS. Cells were then stained with 5.0  $\mu$ g/ml Hoechst 33258 (Sigma) for 2 min, washed to remove unbound dye, and analyzed on a fluorescence plate reader at wavelength filters 360/40 and 460/40.

#### *Western blot analysis*

Cells were lysed in buffer (1% Triton X-100, 50 mM Hepes pH 7.4, 150 mM NaCl, 1.5 MgCl<sub>2</sub>, 1 mM EGTA, 10 mM NaF, 100 mM NaP<sub>i</sub>, 10% glycerol, 1 mM PMSF, 1 mM Na<sub>3</sub>VO<sub>4</sub> and 10  $\mu$ g/ml aprotinin) and protein concentration was measured with the Bio-Rad protein assay kit. To analyze ZNF217 and the HA tag, proteins (50  $\mu$ g) were separated on 8% SDS-PAGE gels followed by transfer onto nitrocellulose membranes. After blocking for 30 min with 5% nonfat dried milk, blots were probed at room temperature with rabbit polyclonal antibody to ZNF217 (Dr. P. Yaswen, Lawrence Berkely Laboratory, Berkely, CA) at a 1:500 dilution for 3 hr, or with mouse anti-HA monoclonal antibody GO36 (Applied Biological Materials, Vancouver, Canada) at a 1:1,000 dilution for 1 hr. After extensive washing with TBST, the immune complexes were detected with horseradish peroxidase conjugated goat anti-rabbit or goat anti-mouse secondary antibodies (1:2,500, Bio-Rad Laboratories, Hercules, CA) for 1 hr followed by ECL (BioLynx, Brockville, ON, Canada). To demonstrate total and phosphorylated Akt and ERK1/2, protein was processed as earlier but was separated on 10% SDS-PAGE gels, and the blots were probed overnight with mouse monoclonal antibody against phosphorylated p44/42 MAP kinases (pERK1/2), rabbit polyclonal antibodies against p44/42 MAP kinases (ERK1/2), phosphorylated Akt and Akt (all from Cell Signaling Technology, Beverly, MA) at a 1:1,000 dilution.

### ZNF217 gene-specific siRNA assays

Exponentially growing IOSE-144RZ cells were seeded at 70% density for 24 hr. Then, the cells were transfected with ZNF217 gene specific siRNAs (Smart-pool<sup>TM</sup>, Dharmacon Research, Lafayette, CO) at concentrations of 30, 40 and 50 nM using Lipofectamine 2000 (Invitrogen). The transfected cells were incubated overnight before being trypsinized, counted and assayed for anchorage independent growth. After 7 days of incubation, colonies were counted. Both the transfection reagent and siRNA scramble controls were included. Changes in growth and morphology associated with the ZNF217 siRNA assay were also examined with cells that were transfected with siRNA and maintained under standard conditions for 1–4 days posttransfection.

### Telomerase assays

Telomerase activity was measured using both TRAPeze Telomerase detection systems (Chemicon International, Temecula, CA) and the Telo TAGGG Telomerase PCR ELISA assay (Roche Diagnostics, Laval, QC, Canada) according to the manufacturer's instructions. Telomere length measurements were carried out as described previously.<sup>25</sup> Briefly, the Telorette 3 oligonucleotide was ligated to chromosome ends by virtue of a 7-bp sequence complimentary to the 3' overhang of telomeric DNA. Long PCR was then conducted using a primer specific for the Telorette 3 sequence (TelTail) and a primer in the telomere-adjacent region of Xp/Yp, 407 bp from the start of the telomere (XpYpE2). Amplicons were resolved on agarose and detected by Southern Blotting and hybridization to a probe specific for the Xp/Yp telomere-adjacent region. The primers were as follows:

Telorette 3; 5'-TGCTCCGTGCATCTGGCATCCCTAAC-3'  
 TelTail 5'-TGCTCCGTGCATCTGGCATC-3'  
 XpYpE2 5'-TTGTCTCAGGGTCCTAGTG-3'  
 XpYpB2 5'-TCTGAAAGTGGACC(A/T)ATCAG-3' (together with XpYpE2 makes up probe).

Since EGF/HC was used in some experiments in conjunction with ZNF217 transduction, we also determined whether EGF/HC alone would activate telomerase in IOSE cells.<sup>26</sup>

Quadruplicate cultures of the parent lines IOSE-80 and IOSE-144 and low passage OSE maintained on EGF/HC for several passages were grown to 90% confluence, changed to serum-free medium, and 24 hr later treated with serum-free medium with/without EGF/HC. After 24 hr, the cells were processed by the Roche assay for telomerase activity as described earlier.

### Tumorigenicity assay

Six- to eight-week-old female SCID mice (Charles River, Wilmington, MA), 3 animals per group, were injected i.p. with  $5 \times 10^6$  cells in 300  $\mu$ l medium. Cells were IOSE-144 at passage 12 or ZNF217-HA-transduced IOSE-144RZ (see later) at passage 56. After 4 months, the animals were killed and examined for tumor formation.

### Statistical analysis

The one-way ANOVA test (Tukey) was used for statistical analysis. All statistical evaluations were performed using the Prism statistical software package (GraphPad Software, San Diego, CA).

## Results

### OSE cells in low passage

Eight sets of cultures of normal OSE cells in passages 1–7 (after approximately 1–2 months in culture) were adenovirally infected with ZNF217-HA or a  $\beta$ -galactosidase control vector. Expression of an EGFP adenoviral construct confirmed that infection efficiency was near 100% (data not shown). By immunofluorescence microscopy, the subcellular location of ZNF217-HA depended on

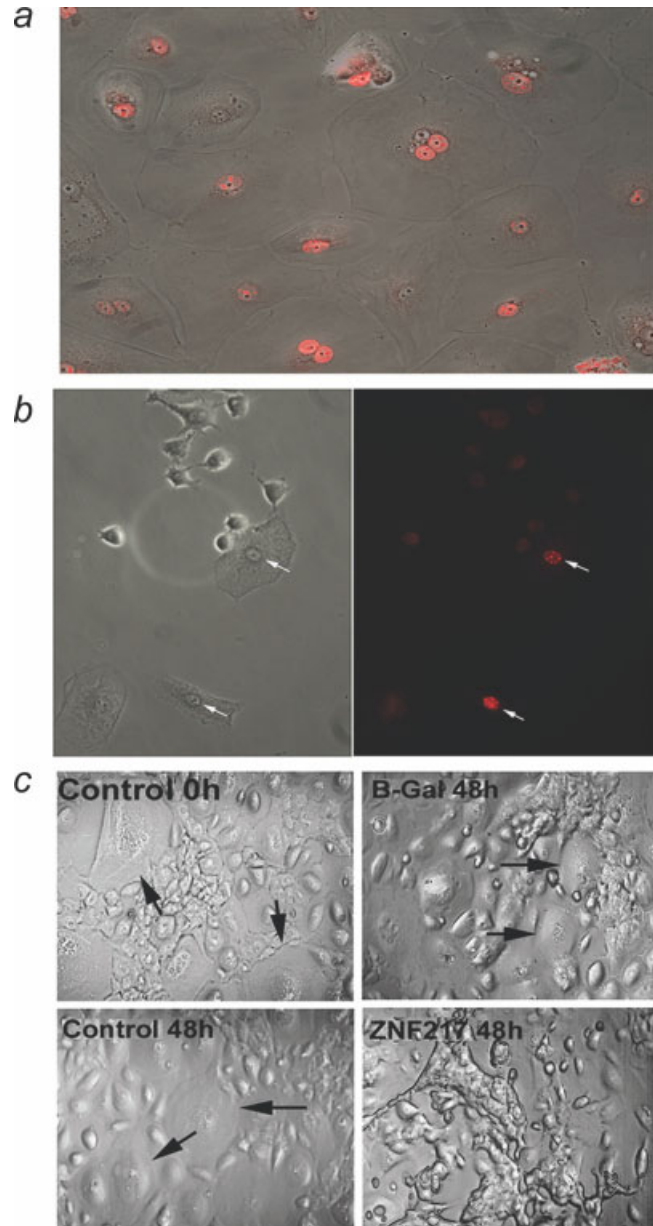


**FIGURE 1** – Immunofluorescence analysis of ZNF217-HA distribution and morphology of low passage OSE cells infected adenovirally with ZNF217-HA. (a,b) Merged phase and IF images; (a) the HA-tagged ZNF217 (red fluorescence) is localized in most nuclei in a culture where cells are stationary and senescent, as indicated by large size, flat shapes and binucleation. (b) In a mixed culture of proliferating and stationary cells, nuclear HA tag is detectable only in senescent cells (arrows). (c) Phase microscopy of a culture grown in parallel with the culture in Figure 1b, composed of a mixture of small proliferating cells and large flat senescent cells (arrows). In cultures infected with ZNF217-HA, the senescent cells have disappeared selectively after 48 hr, while small replicating cells exhibit reduced adhesiveness to plastic.  $\beta$ -gal is a control culture, infected with a  $\beta$ -galactosidase vector, where the senescent cells persist.

the proliferative activity and/or replicative stage of the cells; intense punctate nuclear staining was observed in cells that were senescent as indicated by lack of proliferation, large cell size, flattened cell shapes and multinucleation. In contrast, in younger, proliferating OSE cells and in OSE cells that were proliferating in response to EGF treatment,<sup>27</sup> fluorescence was weakly cytoplasmic or undetectable (Figs. 1a and 1b). Furthermore, ZNF217-HA

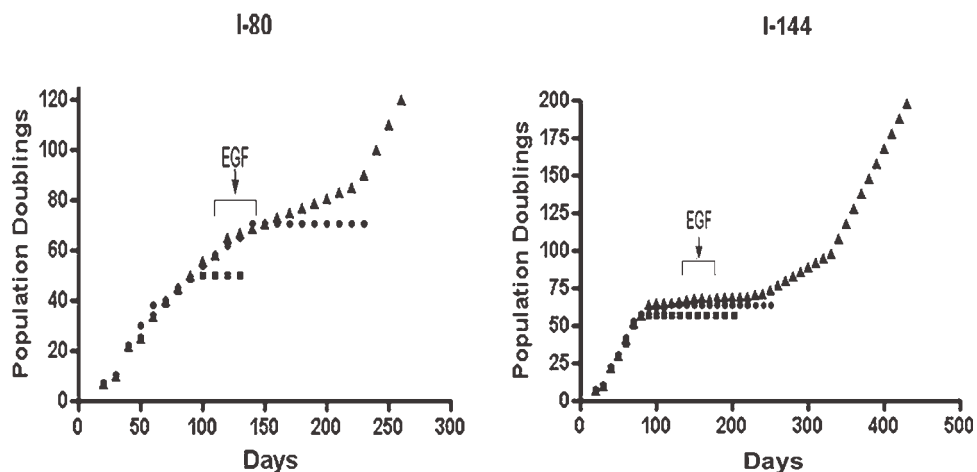


FIGURE 2 – Effects of retrovirally transduced *ZNF217-HA* and EGF/HC on the proliferation of IOSE-80 and IOSE-144 cells. *ZNF217-HA*-transduced cells (■) grew at the same rates and senesced at similar times as the parent lines. Growth in EGF/HC-supplemented medium without *ZNF217-HA* infection (●) delayed crisis by several passages, but did not prevent it. *ZNF217-HA*-transduced cultures, exposed for 3 passages to EGF/HC just prior (IOSE-80) or during (IOSE-144) the time of crisis, gave rise to the EGF-independent, permanent lines I-80RZ and I-144RZ (▲), most likely because EGF/HC treatment extended the life span of the senescent, genomically unstable cell populations at the time of crisis.

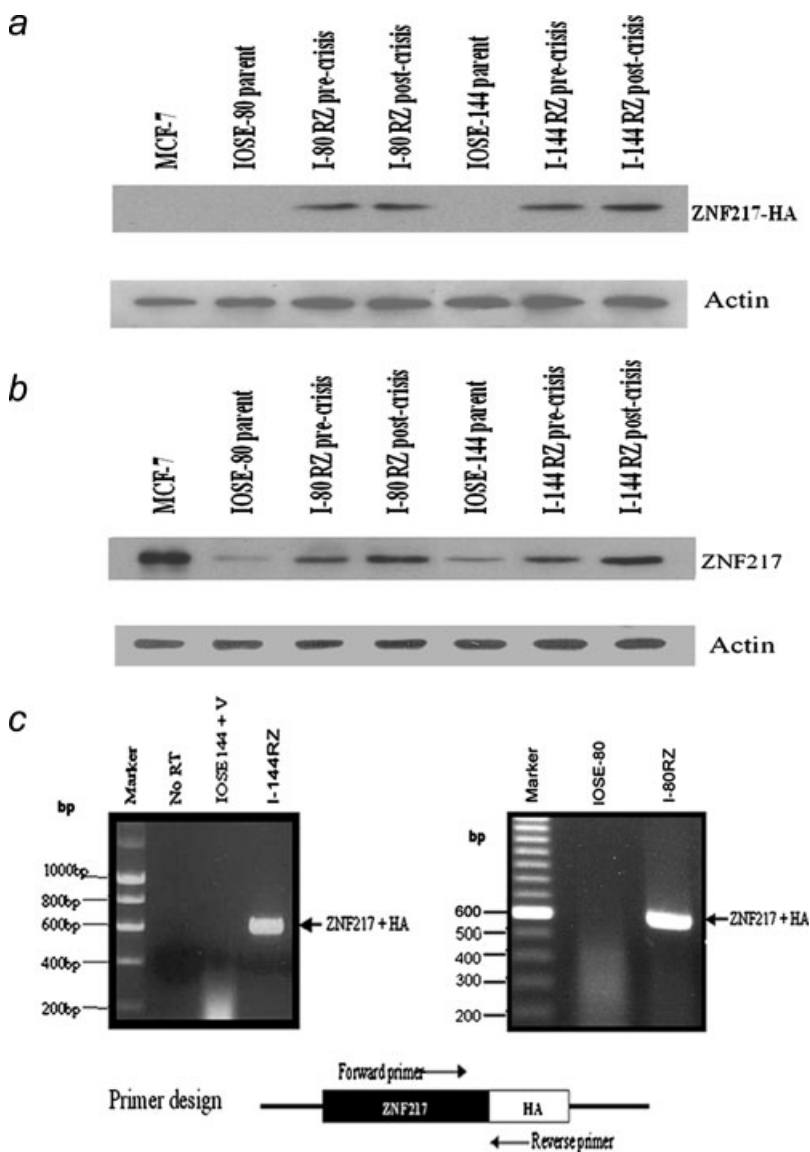


FIGURE 3 – *ZNF217-HA* expression in precrisis IOSE-80 and IOSE-144 cells infected with *ZNF217-HA* and in the postcrisis lines I-80RZ and I-144RZ. (a,b) Western blots: (a) monoclonal antibody G036 reveals HA tag expression in *ZNF217-HA* infected pre- and postcrisis cultures of lines IOSE-80 and IOSE-144 but not in the controls, MCF7 and IOSE parent lines. (b) Rabbit polyclonal antibody to *ZNF217* shows increasing expression of *ZNF217* protein from parent line to precrisis to postcrisis *ZNF217*-transduced lines of IOSE-80 and IOSE-144 cells. The MCF-7 cell line was used as positive control. (c) RT-PCR demonstrates *ZNF217-HA* expression in I-80RZ and I-144RZ, but not in the parent lines or vector control.

did not interfere with growth or cause visible damage when introduced into proliferating cells, while 65–95% of presenescent and senescent cells were dead within 3 days post-infection. In cultures containing both cell types, senescent cells disappeared within few days, while nonsenescent cells retracted partially from plastic but continued to replicate (Fig. 1c). Thus, overexpression of ZNF217-HA accelerated the loss of senescent cells and induced changes in growth pattern indicative of reduced cell-substratum adhesion.

#### IOSE lines

IOSE lines have an extended but finite life span and lack functional p53 and pRb.<sup>20</sup> ZNF217 was introduced into IOSE cells by adenoviral and retroviral infection.

IOSE-120 cells were transiently infected with an adenoviral ZNF217 construct to determine whether a high infection efficiency would cause phenotypic changes. A control EGFP vector indicated near 100% infection efficiency (data not shown). Infection with either adenoviral ZNF217 or vector controls caused no phenotypic changes other than nonspecific transient damage such as detachment and vacuolation, which was similar in both groups. The cultures senesced after about 20 passages as did the controls (data not shown).

Infection with a retroviral vector containing ZNF217-HA produced cells that were G418 resistant, positive for the HA-tag and overexpressed ZNF217 protein, but showed no changes in growth characteristics, were not anchorage independent, and crisis was not delayed or obviated. Like the parent lines and vector controls, the retrovirally infected cells senesced by 15–20 passages (approximately 50 population doublings). Thus, overexpression of ZNF217-HA alone was insufficient to induce immortalization or phenotypic alterations in precrisis IOSE cultures (Fig. 2).

#### Influence of epidermal growth factor/hydrocortisone

EGF/HC acts as a mitogen and delays senescence in low passage OSE cells, with EGF being the crucial component. HC enhances EGF effects, but does not by itself stimulate growth or contribute to immortalization.<sup>27</sup> We hypothesized that EGF/HC might similarly delay crisis in ZNF217-infected IOSE lines and alter the cells' response to ZNF217 overexpression. The culture medium of retrovirally ZNF217-infected IOSE-80 and IOSE-144 cultures was therefore supplemented for 3 passages with 10 ng/ml EGF/HC just prior to crisis (IOSE-80) or at the time of crisis (IOSE-144) (Fig. 2). As mentioned earlier, ZNF217-HA alone did not immortalize the cells; rather they became stationary and senesced around passage 15. Addition of EGF/HC alone to uninfected IOSE lines extended their life span by several passages and population doublings, but then they, too, entered crisis and died. In contrast, cultures infected with retroviral ZNF217-HA and treated with EGF/HC for 3 passages near the time of crisis not only underwent 3–4 additional population doublings before senescence, but a limited number of cells remained in crisis for up to 3 months, when rare colonies of proliferating cells appeared, which were independent of EGF for unlimited growth. The colonies of each line were pooled, and each resulting polyclonal cell line was identified with the prefix 'I' for IOSE, and the suffix 'RZ', for 'retroviral ZNF217'. In both I-80RZ and I-144RZ cells, RT-PCR and immunoblotting demonstrated ZNF217-HA message and ZNF217-HA protein (Fig. 3). Both lines have undergone over 50 passages (more than 120 population doublings), and thus are considered as permanent.

As shown in Figures 4a and 4b, EGF activation of Akt and ERK1/2 in precrisis ZNF217-HA infected IOSE cells was inhibited by the PI3K inhibitor LY294002 and the MAPK/ERK inhibitor PD98059, respectively. EGF appeared to enhance the proliferation, and consequently the lifespan, of these cultures predominantly *via* activation of the PI3K pathway rather than the MAPK pathway, because addition of LY294002 arrested growth and initiated senescence, while the effects of PD98059 were relatively minor (Figs. 4c and 4d).

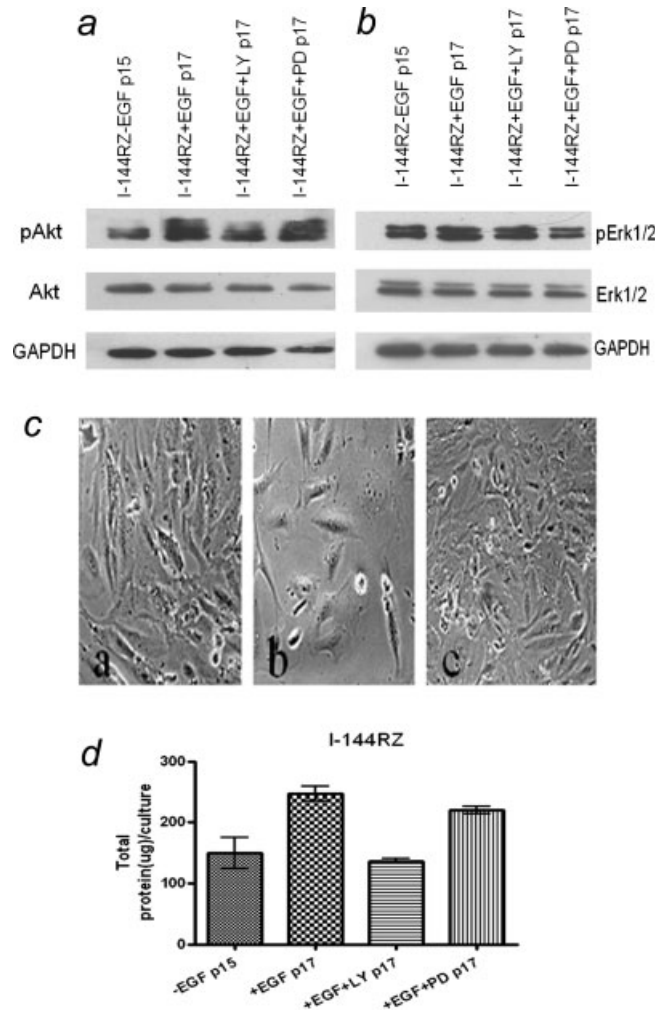


**FIGURE 4** – Signaling pathways mediating the effect of 3 days of EGF/HC treatment on precrisis ZNF217-infected cells. (a) EGF/HC-induced activation of Akt is inhibited by LY294002, while (b) ERK1/2 activation by EGF/HC is inhibited by PD98059. (c) Phase micrographs: untreated control cells (a) and PD98059-treated cells (c) resemble one another morphologically and proliferate in the presence of EGF/HC, while LY294002-treated cells (b) are growth arrested and exhibit morphologic features of senescence. (d) LY294002 arrested growth over 3 days of EGF/HC treatment, while PD98059 did not; mean and range of duplicate cultures.

#### CGH and affymetrix analysis

Minimal amplified/deleted genomic regions were defined with array CGH data from either the I-144RZ or I-80RZ line, which ever had smaller regions (Fig. 5, Supplement 1, online). Genes with more than 2-fold of expression levels in the amplified regions or less than 0.5 fold in the deleted regions of either ZNF217-HA transduced line compared to the expression levels of control cell lines are listed in Table I and Supplement 1 (online). Array CGH analysis showed gains on 3q13-28, 8q24, 14q24 in I-144RZ and on 4p15, 6q, 9, 17p11-13, 20q11-13 in I-80RZ, while copy numbers were reduced in both lines at 18p11-q23 and Xq21-q22, and in I-144RZ at 3p21-14, 7q21 and 13q22 (Fig. 5). There was a striking resemblance between genomic aberrations formed during ZNF217-immortalization and recurrent low-level abnormalities in ovarian tumors. Of particular interest were gene deletions in both cell lines on chromosomes 18 and X, as well as the amplifications at 3q in line I-144RZ and at 20q in line I-80RZ, both of which are among the most frequent and important amplicon sites in ovarian carcinomas.

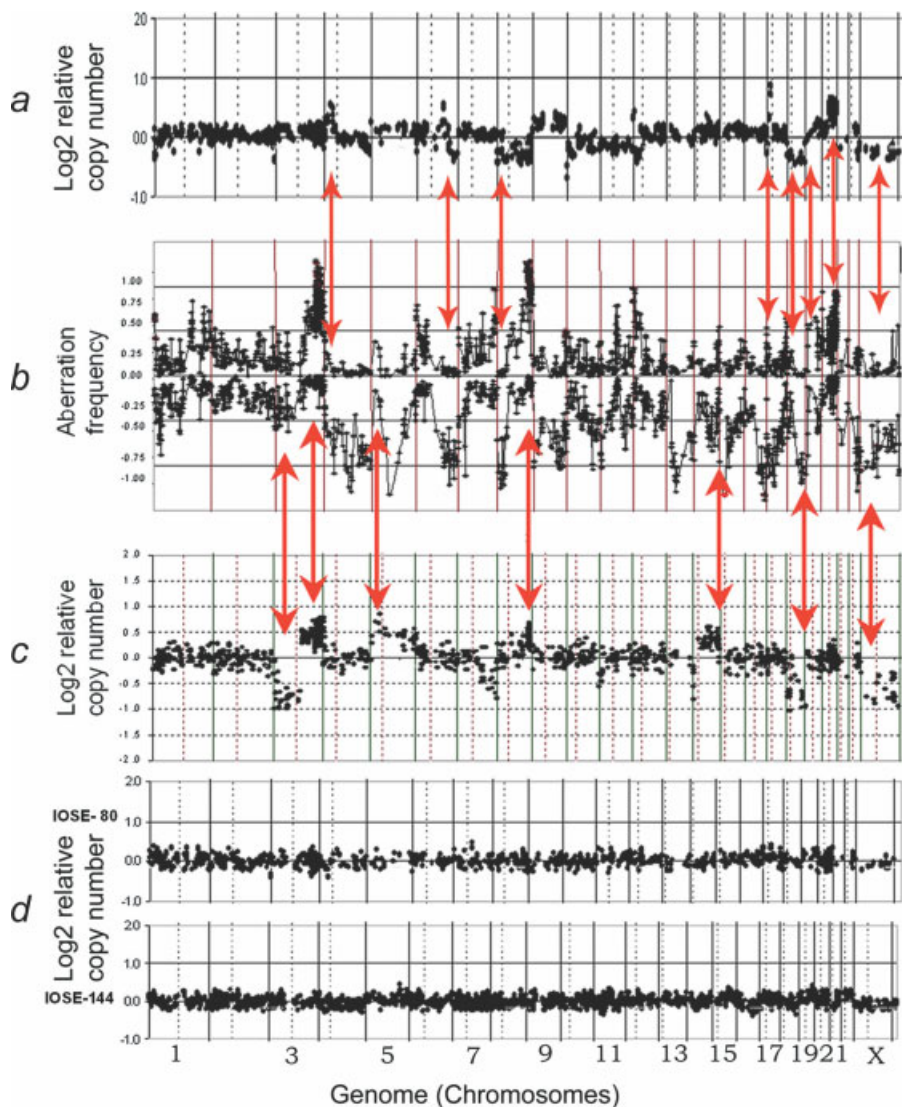


**FIGURE 5** – Low level genomic aberrations formed during ZNF217-IOSE passage through crisis in the ZNF217-HA-transduced lines I-80RZ and I-144RZ match recurrent low-level abnormalities in ovarian tumors. Array CGH analysis of gene copy numbers; CGH ratios are arranged from short arm to long arm and from chromosome 1 to chromosome 22, then X. (a) aberrations in line I-80RZ; (b) aberration frequencies in the genomes of 225 serous ovarian tumors; (c) aberrations in line I-144RZ. (d) Parent line controls prior to infection with ZNF217. In panels a, c and d, genome copy numbers are shown as log<sub>2</sub> relative copy numbers on the Y-axis. In panel b, positive values indicate frequencies of copy number increases, and negative values indicate frequencies of copy number decreases.

The Affymetrix expression arrays were analyzed for 2-fold or greater changes in gene expression that occurred in both I-80RZ and I-144RZ. None of the genes that were overexpressed by these criteria paralleled gene amplifications; however, 8 underexpressed genes localized to deleted chromosome regions (Table I; Supplement 1, online). These included *ANXA10* on 4q and *YES1*, *FLJ12542*, *GATA6*, *CDH2*, *DSC3*, *SCOP* and *SERPINB2*, all on chromosome 18. Importantly, of these 8 gene products, 4 have been implicated in tumor suppression: Annexin A10,<sup>28</sup> desmocollin 3,<sup>29</sup> PAI2,<sup>30</sup> and N-cadherin.<sup>31</sup> N-cadherin is also the major intercellular adhesion molecule of normal OSE.<sup>19</sup> The expression of many other genes was increased or decreased 2-fold or more in one or both lines, unrelated to gene amplifications and deletions, presumably by epigenetic means. Table I lists some of the genes that were altered in both lines, and which may have contributed to their neoplastic progression. They included increased expression of the translation elongation factor and oncogene, *EEF1A2*, and of *STAT1* and *SMAR3*. In contrast to the small number of overexpressed genes, expression of many more genes was reduced in both lines. These included the oncogenes *RAB31* and *v-YES1*, TGF- $\beta$  family members, the tumor suppressors listed earlier and several extracellular matrix, cytoskeleton- and adhesion-related gene products.

#### Phenotypic analysis

Line I-144RZ showed only weak to moderate cytoplasmic staining for ZNF217-HA; nuclei were unstained for HA tag (Fig. 6a). Telomerase activity was absent in the parent line and vector control, but present in I-144RZ (Fig. 6b). As expected, telomere lengths were reduced at crisis compared to the parent line at earlier passages, but their lengths increased with time after crisis, to levels similar to the parent line (Table II). I-144RZ was more serum-independent and replicated even in the complete absence of serum and was anchorage independent while the parent line formed no colonies (Figs. 6c and 6d). Changes in gene expression, based on Affymetrix analysis, which may have contributed to anchorage independence, were a 2.0-fold increase in EGF receptor expression and a 5.6-fold reduction in the expression of TGF $\beta$ 2. siRNA to ZNF217 mRNA completely arrested proliferation and inhibited anchorage independence. The scramble controls had lesser and reversible effects (Fig. 7).

Line I-80RZ also survived crisis under the combined influence of ZNF217 and EGF/HC and subsequently proliferated without EGF/HC (Fig. 2). ZNF217-HA expression was confirmed by RT-PCR and Western blots (Fig. 3). By immunofluorescence, protein was undetectable or weakly cytoplasmic. Telomerase activity was expressed in I-80RZ but not in the parent line (Fig. 6b) and telomere

**TABLE 1 – OVER- OR UNDEREXPRESSED GENES, SELECTED FROM AFFYMETRIX EXPRESSION ARRAYS BY RELEVANCE TO NEOPLASTIC PROGRESSION**

Gene symbol	Gene description	Fold change from control <sup>1</sup>	
		I-80RZ	I-144RZ
<b>Increased expression</b>			
EEF1A2	Eukaryotic translation elongation factor 1 alpha 2	3.4	4.4
SMARCA3	SWI/SNF related, matrix associated, actin dependent regulator of chromatin	2.7	2.7
STAT1	Signal transducer and activator of transcription 1	3.3	4.3
<b>Decreased expression</b>			
<b>Oncogenes, tumor suppressors</b>			
RAB31	RAB31, member RAS oncogene family	-3.1	-3.4
<b>YES1</b>	<b>V-YES-1 Yamaguchi sarcoma viral oncogene homolog 1</b>	<b>-2.5</b>	<b>-2.1</b>
RIS1	Ras-induced senescence 1	-10.6	-7.7
THBS1	Thrombospondin	-2.5	-10.0
ACTA	Activin A	-24.9	-3.3
TGFBR2	TGF beta receptor 2	-3.0	-3.5
<b>Extracellular matrix components, proteases, protease inhibitors</b>			
<b>SERPINB2</b>	<b>Serine (or cysteine) proteinase inhibitor</b>	<b>-3.3</b>	<b>-31.6</b>
COL3A1	Collagen type III alpha 1	-2.6	-71.8
COL5A1	Collagen type V alpha 1	-2.0	-2.3
DCN	Decorin	-2.3	-5.0
FN	Fibronectin	-2.2	-3.4
MMP2	Matrix metalloproteinase 2	-2.7	-5.8
TIMP3	Tissue inhibitor of metalloproteinase 3	-6.7	-4.9
<b>Cell adhesion, cytoskeleton</b>			
<b>DSC3</b>	<b>Desmocollin 3</b>	<b>-3.2</b>	<b>-2.5</b>
<b>CDH2</b>	<b>Cadherin 2, type 1, N-cadherin (neuronal)</b>	<b>-3.2</b>	<b>-3.1</b>
CAV2	Caveolin 2	-2.3	-2.2
CDH11	Cadherin 11, type 2, OB-cadherin (osteoblast)	-61.0	-22.3
ACTA2	Actin, alpha 2, smooth muscle, aorta	-2.1	-3.1
KRT19	Keratin 19	-137.8	-2.6
<b>Others</b>			
<b>FLJ12542</b>	<b>Hypothetical protein FLJ12542</b>	<b>-2.7</b>	<b>-2.8</b>
<b>ANXA10</b>	<b>Annexin 10</b>	<b>-41.1</b>	<b>-2.8</b>
<b>GATA6</b>	<b>GATA binding protein 6</b>	<b>-11.0</b>	<b>-14.8</b>
<b>SCOP</b>	<b>SCN circadian oscillatory protein (SCOP)</b>		<b>-2.3</b>
RALBP1	ralA binding protein 1	-4.2	-2.1
CALR	Calreticulin	-3.50	-2.0
TFPI2	Tissue factor pathway inhibitor 2	-10.4	-4.5
TSG	Twisted gastrulation	-4.2	-2.0

Two-fold or greater changes in gene expression, associated with genes that are amplified or deleted in both lines I-80RZ and I-144RZ by array CGH are listed in **bold**; other genes, that are transcriptionally up- or downregulated in both lines are in ordinary type.

<sup>1</sup>Controls: average of IOSE-144 and IOSE-144vector control, and IOSE-80, respectively.

lengths increased after crisis (Table II). I-80RZ cells grew more slowly than the parent line; however, they reached higher saturation densities and were more serum independent in that they proliferated in the complete absence of serum (Fig. 6c). I-80RZ cells were also significantly more anchorage independent than the parent line (Fig. 6d). Changes in gene expression that may have contributed to anchorage independence included 2.6–5.4-fold increases in the expression of amphiregulin, laminin alpha 5, and integrin beta 4, as shown by Affymetrix analysis. As in the I-144RZ line, siRNA to *ZNF217* arrested proliferation and reduced anchorage independence (Fig. 7). Over a 4-month period, neither I-144RZ cells nor I-80RZ cells formed tumors or caused ascites in SCID mice.

Since the cells had been transiently treated with EGF during crisis, and since it has been reported that EGF can induce telomerase activity directly,<sup>26</sup> we investigated whether EGF/HC alone, without *ZNF217*, would activate telomerase in our system. No telomerase activity was detected in response to EGF/HC stimulation in either low passage OSE cells or in the parent lines IOSE-80 and IOSE-144 (data not shown).

## Discussion

Our study shows that *ZNF217* promoted the neoplastic progression of human OSE by introducing 4 important malignancy-associated characteristics: immortality, telomerase activity, reduced serum dependence and anchorage independence. In view of the re-

semblance of the *ZNF217*-induced genomic aberrations and changes in gene expression to common aberrations observed in ovarian carcinomas, these cell lines represent a unique model to investigate relationships between genomic and phenotypic aspects of ovarian epithelial neoplastic progression.

Our results supplement those of Nonet *et al.*<sup>17</sup> who demonstrated a similar influence of *ZNF217* on human mammary epithelial cells. In both cases, constitutively active *ZNF217* was introduced into precrisis cell lines with defective proliferative controls: the mammary cells lacked functional p16<sup>INK4a</sup>, while the IOSE lines lacked functional p53 and pRB. In both systems, the target cells had extended, but limited lifespans compared to normal cells. Introduction of *ZNF217* was followed by telomerase activation and an apparently indefinite proliferative potential in both systems.

Our CGH data and expression arrays provide new information about possible mechanisms involved in *ZNF217*-mediated neoplastic progression and extend them specifically to ovarian carcinogenesis. In particular, our study identified changes in gene expression associated with *ZNF217* overexpression, which include downregulation of several tumor suppressors and overexpression of oncogenes, including *EEF1A2*, which is frequently amplified in ovarian cancer. In addition to phenotypic changes reported for the mammary system, we demonstrated that *ZNF217* induces anchorage independence and serum independence, both suggestive of activation of autocrine growth promoting factors and confirmed the *ZNF217*-dependence of such neoplastic progression by siRNA assays. Importantly,

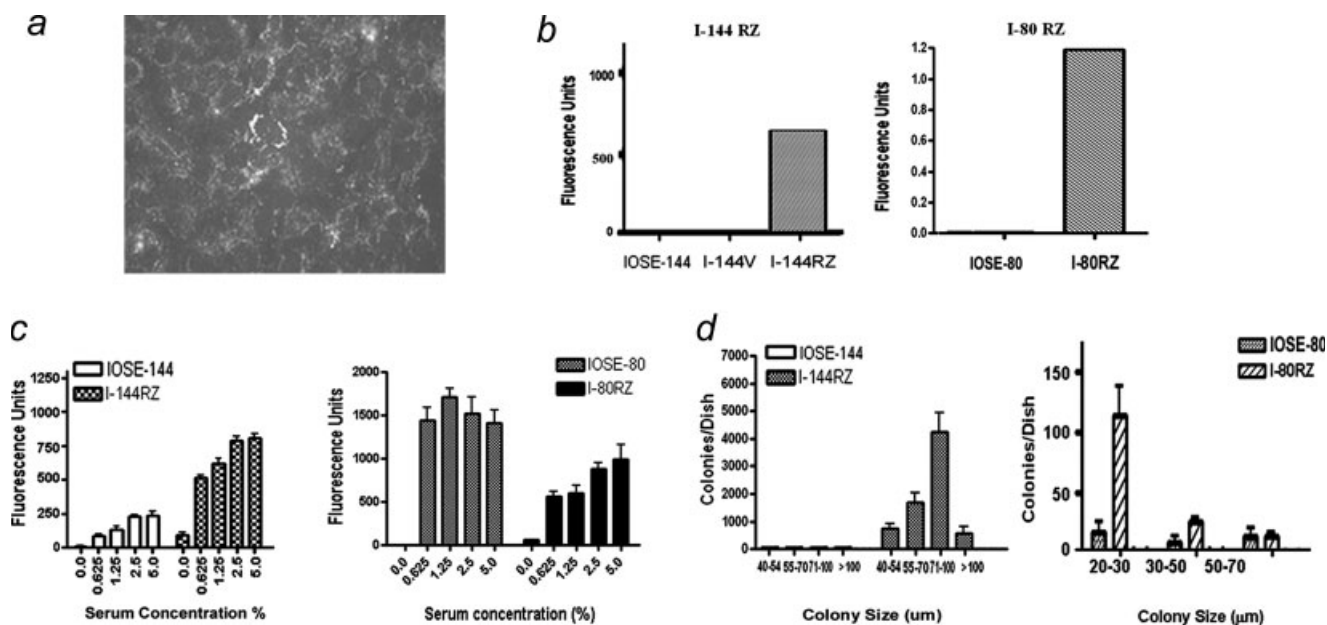


**FIGURE 6** – Phenotypic characteristics of lines I-144RZ and IOSE-80RZ. (a) *ZNF217-HA* distribution in line I-144RZ. The fluorescence is mainly cytoplasmic. (b) Telomerase activity is detected only in the *ZNF217-HA*-expressing lines but not in the parent lines or in the vector control I-144V. (c) Serum and anchorage dependence: at all serum concentrations, line I-144RZ is significantly less serum dependent ( $p < 0.05$ ) than the parent line and proliferates even in the complete absence of serum. I-80RZ cells grow more slowly than IOSE-80 cells, but in contrast to IOSE-80, they also proliferate without any serum, indicating increased serum independence. Mean and SD of 6 replicates/serum concentration, collected after 9 days. (d) Anchorage independence: over 20 days, the parent lines, IOSE-144 and IOSE-80 formed no or few colonies in agarose while lines I-144RZ and I-80RZ produced significantly more colonies ( $p < 0.01$  for total number of colonies, in both lines). Mean and SD of 3 cultures per group.

**TABLE II** – SIZE VARIATION OF XP/YP TELOMERE LENGTHS BETWEEN PARENT LINES AND RETROVIRALLY *ZNF217-HA*-INFECTED IOSE CELL LINES (I-80RZ AND I-144RZ) AT VARIOUS PASSAGES

Cell line	Stage	Passage	Telomere activity	No. of Xp/Yp telomeres analyzed	Mean telomere length (kb)
IOSE-80	Parent line	12	–	84	2.18 ± 0.13
I-80RZ	Postcrisis	26	++	151	1.33 ± 0.06
I-80RZ	Postcrisis	36	++	98	1.91 ± 0.09
I-144	Parent line	17	–	178	2.88 ± 0.31
I-144RZ	Postcrisis	27	++	176	1.23 ± 0.08
I-144RZ	Postcrisis	58	++	150	2.64 ± 0.2

by comparing low passage and SV40Tag/tag-immortalized cells, we defined, for the first time, major differences in the cellular responses to *ZNF217* depending on the state of p53 and pRB.

The ovarian IOSE cell lines lack functional p53 and pRB, 2 of the principal regulators of cell proliferation and senescence. Both telomeric and nontelomeric signals induce cell cycle arrest and senescence in human cells *via* the p53-p21-pRB pathway (reviewed in ref. 32). It was shown previously that inactivation of p53 and pRB extends the life span of ovarian epithelial cells in culture<sup>20</sup> and contributes to ovarian tumorigenicity *in vivo*.<sup>33,34</sup> Furthermore, p53 is the most commonly inactivated tumor suppressor in ovarian cancers. In contrast, p53 was not inactivated in the mammary system and pRB was not investigated.<sup>17</sup> Interestingly though, the mammary cells lacked functional p16<sup>INK4a</sup>, which is an upstream regulator of both p53 and pRB and interferes with pRB function *via* an alternate pathway.<sup>32</sup> Together, the results of the two studies suggest that hypophosphorylation of pRB as well as p53 may be contributing factors in *ZNF217*-mediated immortalization and neoplastic progression.

Our observations on freshly explanted OSE cells represent the first available information on effects of *ZNF217* overexpression on cells with normal genomes. *ZNF217* accelerated the death of OSE cells approaching senescence and interfered with cell adhesion, which may reflect the reduced expression of several adhe-

sion-related genes (Table I, online supplement 1). There is increasing evidence that oncogenes can promote senescence in normal cells, and this response has been interpreted as representing a natural barrier to tumorigenesis.<sup>32</sup> Importantly, this defense mechanism depends on either or both the tumor suppressor proteins p53 and p16<sup>INK4a</sup>. The deleterious effect of *ZNF217* overexpression on normal OSE cells with their wild type p53 and pRB, and the opposite, immortalizing effect on the p53, pRB-deficient IOSE cells is strikingly similar to the inverse effects of, *e.g.*, activated H-RAS on primary vs. p53-deficient human cells.<sup>32,34</sup>

In precrisis IOSE cultures, EGF alone delayed crisis but did not prevent it, in keeping with previous results.<sup>35,36</sup> However, brief EGF treatment during crisis in conjunction with overexpressed *ZNF217* allowed cells to overcome crisis and to acquire additional neoplastic features. EGF acts as a mitogen, promotes survival and delays senescence *via* activation of the PI3K and MAPK pathways.<sup>36</sup> Our results confirmed that EGF treatment extended the life-span of *ZNF217*-infected precrisis IOSE cells by several population doublings. Furthermore, this change was based, at least in part, on an increased proliferative potential which, in turn, depended on activated PI3K. The resulting extended life span of IOSE cultures approaching senescence, which is a period of genetic instability, most likely increased the chance for random genetic changes which predisposed the cells to *ZNF217*-mediated immortalization.

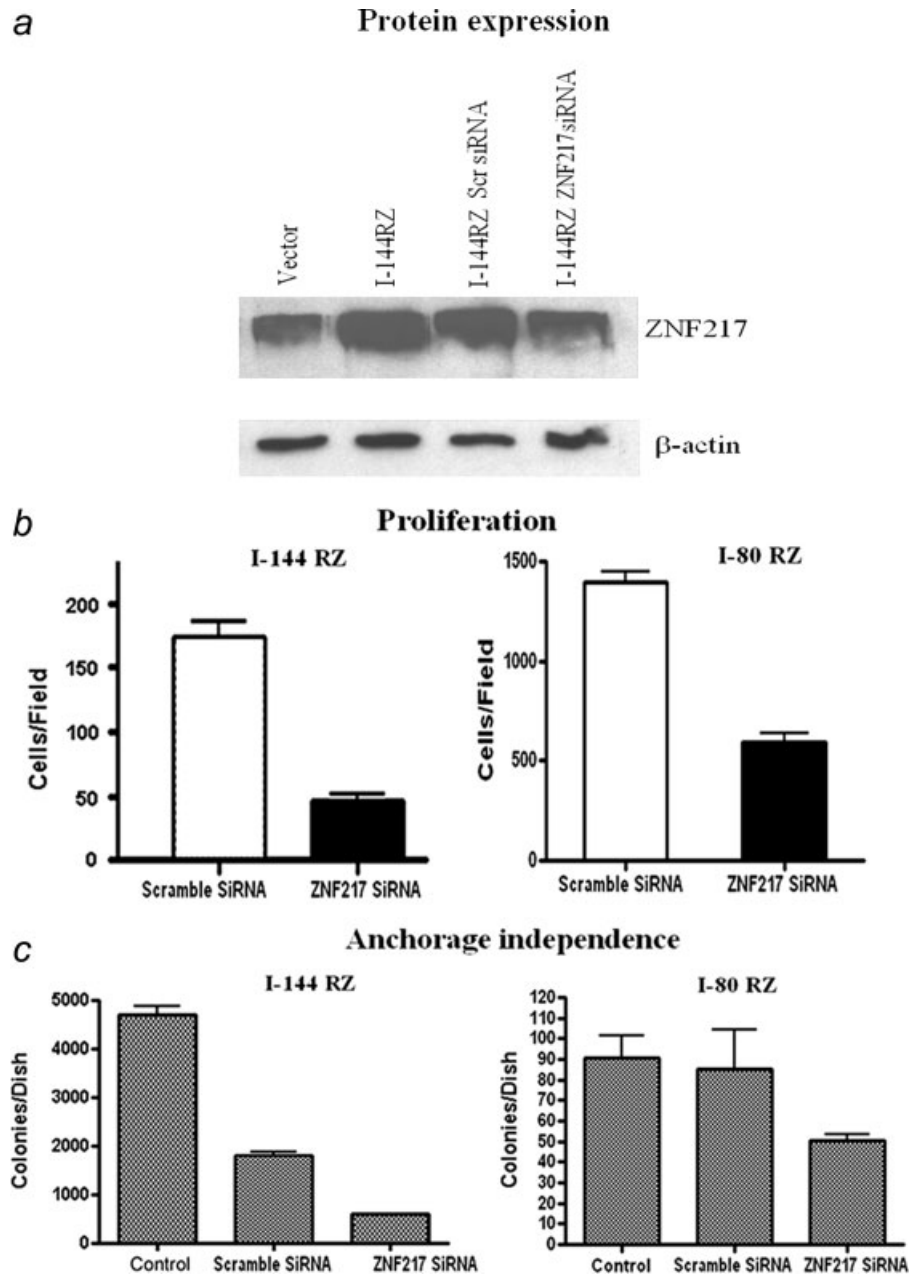


**FIGURE 7** – Effects of 30 nM ZNF217-siRNA adenovirally infected into I-144RZ and I-80RZ cells. (a) Western blot demonstrating reduced ZNF217 protein expression in the presence of siRNA. (b) In both lines, siRNA significantly reduced cell proliferation, while the scramble control cells recovered from infection damage. (c) In both lines, siRNA significantly inhibited colony formation in agarose compared with controls and scramble siRNA ( $p < 0.01$  for I-144RZ,  $p < 0.05$  for I-80RZ). The reduced number of I-144RZ colonies with scramble siRNA is interpreted as due to transfection damage. Mean and SD of 3 cultures per group.

In contrast to the EGF-independence of the postcrisis lines I-80RZ and I-144RZ, which suggests activation of autocrine regulatory mechanisms,<sup>37</sup> anti-ZNF217 siRNA resulted in the rapid cessation of proliferation, demonstrating that ZNF217 was an essential component leading to the acquisition of a permanent life span. Activation of hTERT is an early event in most malignant tumors and contributes to the establishment of permanent cell lines. Although it has been reported that EGF can directly activate hTERT transcription,<sup>26</sup> our present investigation produced no evidence of telomerase activation by EGF alone. The siRNA effect may be related to interference with ZNF217-induced telomerase activity, since telomerase has been shown to maintain proliferation.<sup>38</sup>

Array CGH revealed amplifications at 3q, 8q and 20q and deletions at 3p and 18q, all of which are common in ovarian cancer.<sup>39</sup> Both lines exhibited deletions on 18 and X. In both lines, Affymetrix expression arrays revealed reduced expression of 4 genes with tumor suppressor activity that are located in the deleted region on 18q (*ANXA10*, *CDH2*, *DSC3* and *SCOP*), as well as downregu-

lated expression of the tumor suppressors thrombospondin, TIMP3 and members of the TGF $\beta$  family. Increased gene expression included overexpression of *EEF1A2*, a known ovarian cancer oncogene which, like ZNF217, resides on chromosome 20q13,<sup>40</sup> and of *SMAR3* and *STAT1*, which have also been implicated in neoplastic progression. On the other hand, expression of several genes that enhance neoplastic progression in other systems was downregulated, including *SERPINB2*, *YES1* and *MMP2*, suggesting that activation of these genes does not play a role in ZNF217-mediated transformation.

Anchorage independence is one of the best *in vitro* indicators of neoplastic progression, though it is not always paralleled by tumorigenicity. It requires reduced dependence on normal interactions with the extracellular matrix, which is promoted by substituting autocrine ECM products, matrix and growth factor secretion and by changes in integrin composition and action.<sup>41</sup> The reduced serum dependence of I80RZ and I-144RZ and the altered expression of many extracellular matrix- and adhesion-related proteins

and growth factors (Table I) point to such autocrine regulatory mechanisms. ZNF217 overexpression did not result in tumorigenicity. There are other indications that disruption of the p53 and RB pathways by SV40 large T antigen and small T antigen plus hTERT activation are insufficient to render OSE cells tumorigenic.<sup>34</sup> Therefore, our findings suggest that, although ZNF217 is an important determinant of ovarian neoplastic progression, the acquisition of tumorigenesis seems to involve interactions with additional factors.

A topic requiring further study is the varying subcellular distribution of ZNF217-HA. In cultures of normal OSE, ZNF217-HA was undetectable or detectable at low levels in the cytoplasm of proliferating cells, but was prominent in the nuclei of stationary, senescent cells. The nuclear accumulation of ZNF217 seemed to accelerate cell detachment and death, perhaps by acting as a transcriptional repressor.<sup>18,42</sup> In contrast, ZNF217-HA was cytoplasmic in proliferating OSE cells, in I-144RZ and I-80RZ cells, and in several ovarian cancer lines that were transiently transduced with ZNF217-HA (data not shown), suggesting that its localization may depend on the cells' proliferative state. Whether ZNF217 is

stored and/or has alternate functions in the cytoplasm, as reported for other transcription factors,<sup>42</sup> remains to be determined. Possible relationships of its subcellular distribution to mechanisms of oncogene-induced senescence<sup>32</sup> represent another topic for future investigations.

Taken together, this study supports other evidence for the oncogenic potential of ZNF217 and indicates that ZNF217 likely contributes to neoplastic progression in epithelial ovarian cancer. The I-144RZ and I-80RZ lines represent the first available experimental model to study the mechanisms involved in this process in human OSE-derived cells.

### Acknowledgements

We thank Dr. P. Yaswen, Laurence Berkeley Laboratories, for providing the HA-tagged ZNF217 minigene, empty vector control, and polyclonal antibody to ZNF217. We are grateful to Dr. Peter Lansdorp for his advice regarding telomere length determinations. We greatly appreciate the advice and help of Ms. Clara Salamanca, Ms. Michelle Woo and Mr. Qiang Feng.

### References

- Collins C, Volik S, Kowbel D, Ginzinger D, Yistra B, Cloutier T, Hawkins T, Predki P, Martin C, Wernick M, Kuo W-L, Alberts A, et al. Comprehensive genome sequence analysis of a breast cancer amplicon. *Genome Res* 2001;11:1034-42.
- Collins C, Rommens JM, Kowbel D, Godfrey T, Tanner M, Hwang SI, Polikoff D, Nonet G, Cochran J, Myambo K, Jay KE, Froula J, et al. Positional cloning of ZNF217 and NABC1: genes amplified at 20q13.2 and overexpressed in breast carcinoma. *Proc Natl Acad Sci USA* 1998;95:8703-8.
- Bar-Shira A, Pinthus JH, Rozovsky U, Goldstein M, Sellers WR, Yaron Y, Eshar Z, Orr-Urtreger A. Multiple genes in human 20q13 chromosomal region are involved in an advanced prostate cancer xenograft. *Cancer Res* 2002;62:6803-7.
- Freier K, Joos S, Flechtenmacher C, Devens F, Benner A, Bosch FX, Lichter P, Hofele C. Tissue microarray analysis reveals site-specific prevalence of oncogene amplifications in head and neck squamous cell carcinoma. *Cancer Res* 2003;63:1179-82.
- Weiss MM, Sniijders AM, Kuipers EJ, Ylstra B, Pinkel D, Meuwissen SO, van Diest PJ, Albertson DG, Meijer GA. Determination of amplicon boundaries at 20q13.2 in tissue samples of human gastric adenocarcinomas by high-resolution microarray comparative genomic hybridization. *J Pathol* 2003;200:320-6.
- Rooney PH, Boonsong A, McFadyen MC, McLeod HL, Cassidy J, Curran S, Murray GI. The candidate oncogene ZNF217 is frequently amplified in colon cancer. *J Pathol* 2005;204:282-8.
- Yang SH, Seo MY, Jeong HJ, Jeung HC, Shin J, Kim SC, Noh SH, Chung HC, Rha SY. Gene copy number change events at chromosome 20 and their association with recurrence in gastric cancer patients. *Clin Cancer Res* 2005;11:612-20.
- Hidaka S, Yasutake T, Takeshita H, Kondo M, Tsuji T, Nanashima A, Sawai T, Yamaguchi H, Nakagoe T, Ayabe H, Tagawa Y. Differences in 20q13.2 copy number between colorectal cancers with and without liver metastasis. *Clin Cancer Res* 2000;6:2712-17.
- Toncheva D, Zaharieva B. Coexistence of copy number changes of different genes (INK4A, erbB-1, erbB-2, CMYC, CCND1 and ZNF217) in urothelial tumors. *Tumour Biol* 2005;26:88-93.
- Shimada M, Imura J, Kozaki T, Fujimori T, Asakawa S, Shimizu N, Kawaguchi R. Detection of Her2/neu, c-MYC and ZNF217 gene amplification during breast cancer progression using fluorescence in situ hybridization. *Oncol Rep* 2005;13:633-41.
- Tanner MM, Grenman S, Koul A, Johannsson O, Meltzer P, Pejovic T, Borg A, Isola JJ. Frequent amplification of chromosomal region 20q12-q13 in ovarian cancer. *Clin Cancer Res* 2003;6:1833-9.
- Watanabe T, Imoto I, Katahira T, Hirasawa A, Ishiwata I, Emi M, Takayama M, Sato A, Inazawa J. Differentially regulated genes as putative targets of amplifications at 20q in ovarian cancers. *Jpn J Cancer Res* 2002;93:1114-22.
- Ginzinger DG, Godfrey TE, Nigro J, Moore DH, II, Suzuki S, Pallavicini MG, Gray JW, Jensen RH. Measurement of DNA copy number at microsatellite loci using quantitative PCR analysis. *Cancer Res* 2000; 60:5405-9.
- Peiro G, Diebold J, Lohrs U. CAS (cellular apoptosis susceptibility) gene expression in ovarian carcinoma: correlation with 20q13.2 copy number and cyclin D1, p53, and Rb protein expression. *Am J Clin Pathol* 2002;118:922-9.
- Savelieva E, Belair CD, Newton MA, DeVries S, Gray JW, Waldman F, Reznikoff CA. 20q gain associates with immortalization: 20q13.2 amplification correlates with genome instability in human papillomavirus 16 E7 transformed human uroepithelial cells. *Oncogene* 1997;14: 551-60.
- Cuthill S, Agarwal P, Sarkar S, Savelieva E, Reznikoff CA. Dominant genetic alterations in immortalization: role for 20q gain. *Genes Chromosomes Cancer* 1999;26:304-11.
- Nonet GH, Stampfer MR, Chin K, Gray JW, Collins CC, Yaswen P. The ZNF217 gene amplified in breast cancers promotes immortalization of human mammary epithelial cells. *Cancer Res* 2001;61:1250-4.
- Huang G, Krig S, Kowbel D, Xu H, Hyun B, Volik S, Feuerstein B, Mills GB, Stokoe D, Yaswen P, Collins C. ZNF217 suppresses cell death associated with chemotherapy and telomere dysfunction. *Hum Mol Genet* 2005;14:3219-25.
- Auersperg N, Wong AS, Choi KC, Kang SK, Leung PC. Ovarian surface epithelium: biology, endocrinology, and pathology. *Endocr Rev* 2001;22:255-88.
- Maines-Bandiera SL, Kruk PA, Auersperg N. Simian virus 40-transformed human ovarian surface epithelial cells escape normal growth controls but retain morphogenetic responses to extracellular matrix. *Am J Obstet Gynecol* 1992;167:729-35.
- Sniijders AM, Nowak N, Seagraves R, Blackwood S, Brown N, Conroy J, Hamilton G, Hindle AK, Huey B, Kimura K, Law S, Myambo K, et al. Assembly of microarrays for genome-wide measurement of DNA copy number. *Nat Genet* 2001;29:263-4.
- Sniijders AM, Fridlyand J, Mans DA, Seagraves R, Jain AN, Pinkel D, Albertson DG. Shaping of tumor and drug-resistant genomes by instability and selection. *Oncogene* 2003;22:4370-9.
- Jain AN, Tokuyasu TA, Sniijders AM, Seagraves R, Albertson DG, Pinkel D. Fully automatic quantification of microarray image data. *Genome Res* 2002;12:325-32.
- Irizarry RA, Hobbs B, Collin F, Beazer-Barclay YD, Antonellis KJ, Scherf U, Speed TP. Exploration, normalization, and summaries of high density oligonucleotide array probe level data. *Bioinformatics* 2003;4:249-64.
- Baird DM, Rowson J, Wynford-Thomas D, Kipling D. Extensive allelic variation and ultrashort telomeres in senescent human cells. *Nat Genet* 2003;33:203-7.
- Maida Y, Kyo S, Kanaya T, Wang Z, Yatabe N, Tanaka M, Nakamura M, Ohmichi M, Gotoh N, Murakami S, Inoue M. Direct activation of telomerase by EGF through Ets-mediated transactivation of *TERT* via MAP kinase signaling pathway. *Oncogene* 2002;21:4071-9.
- Salamanca CM, Maines-Bandiera SL, Leung PC, Hu YL, Auersperg N. Effects of epidermal growth factor/hydrocortisone on the growth and differentiation of human ovarian surface epithelium. *J Soc Gynecol Invest* 2004;11:241-51.
- Liu S-H, Lin C-Y, Peng S-Y, Jeng Y-M, Pan H-W, Lai P-L, Liu C-L, Hsu H-C. Down-regulation of annexin A10 in hepatocellular carcinoma is associated with vascular invasion, early recurrence, and poor prognosis in synergy with p53 mutation. *Am J Pathol* 2002;160:1831-7.
- Klus GT, Rokaesus N, Bittner ML, Chen Y, Korz DM, Sukumar S, Schick A, Szallasi Z. Down-regulation of the desmosomal cadherin desmocollin 3 in human breast cancer. *Int J Oncol* 2001;19:169-74.
- Shimizu T, Sato K, Suzuki T, Tachibana K, Takeda K. Induction of plasminogen activator inhibitor-2 is associated with suppression of invasive activity in TPA, mediated differentiation of human prostate cancer cells. *Biochem Biophys Res Commun* 2003;309:267-71.

31. Hagihara A, Miyamoto K, Furuta J, Hiraoka N, Wakazono K, Seki S, Fukushima S, Tsao MS, Sugimura T, Ushijima T. Identification of 27 5' CpG islands aberrantly methylated and 13 genes silenced in human pancreatic cancers. *Oncogene* 2004;23:8705–10.
32. Dimri GP. What has senescence got to do with cancer?. *Cancer Cell* 2005;7:505–12.
33. Flesken-Nitkin A, Choi KC, Eng JP, Shmidt EN, Nikitin AY. Induction of carcinogenesis by concurrent inactivation of *p53* and *Rb 1* in the mouse ovarian surface epithelium. *Cancer Res* 2003;63:3459–63.
34. Liu J, Yang G, Thompson-Lanza JA, Glassman A, Hayes K, Patterson A, Marquez RT, Auersperg N, Yu Y, Hahn WC, Mills GB, Bast RC, Jr. A genetically defined model for human ovarian cancer. *Cancer Res* 2004;64:1655–63.
35. Davies BR, Steele IA, Edmondson RJ, Zwolinski SA, Saretzki G, von Zglinicki T, O'Hare MJ. Immortalisation of human ovarian surface epithelium with telomerase and temperature-sensitive SV40 large T antigen. *Exp Cell Res* 2003;288:390–402.
36. McClellan M, Kievit P, Auersperg N, Rodland K. Regulation of proliferation and apoptosis by epidermal growth factor and protein kinase C in human ovarian surface epithelial cells. *Exp Cell Res* 1999;246:471–9.
37. Awwad RA, Sergina N, Yang H, Ziober B, Willson JK, Zborowska E, Humphrey LE, Fan R, Ko TC, Brattain MG, Howell GM. The role of transforming growth factor alpha in determining growth factor independence. *Cancer Res* 2003;63:4731–8.
38. Li S, Rosenberg JE, Donjacour AA, Botchkina AL, Hom YK, Cunha GR, Blackburn EH. Rapid inhibition of cancer cell growth induced by lentiviral delivery and expression of mutant-template telomerase RNA and anti-telomerase short-interfering RNA. *Cancer Res* 2004;64:4833–40.
39. Gray JW, Suzuki S, Kuo WL, Polikoff D, Deavers M, Smith-McCune K, Berchuck A, Pinkel D, Albertson D, Mills GB. Specific keynote: genome copy number abnormalities in ovarian cancer. *Gynecol Oncol* 2003;88:S16–S21.
40. Anand N, Murthy S, Amann G, Wernick M, Porter LA, Cukier IH, Coll C, Gray JW, Diebold J, Demetrick DJ, Lee JM. Gene encoding protein elongation factor EEF1A2 is a putative oncogene in ovarian cancer. *Nat Genet* 2002;31:301–5.
41. Zahir N, Lakins JN, Russell A, Ming W-Y, Chatterjee C, Rozenberg GI, Marinkovich MP, Weaver VM. Autocrine laminin-5 ligates alpha6beta4 integrin and activates RAC and NFkappaB to mediate anchorage-independent survival of mammary tumors. *J Cell Biol* 2003;163:1397–407.
42. Soubry A, van Hegel J, Parthoens E, Colpaert C, Van Marck E, Waltrigny D, Reynolds AB, van Roy F. Expression and nuclear location of the transcriptional repressor Kaiso is regulated by the tumor micro-environment. *Cancer Res* 2005;65:2224–33.